THE JOURNAL OF BIOLOGICAL CHEMISTRY VOL. 288, NO. 5, pp. 2914–2922, February 1, 2013
Published in the U.S.A.

Evidence for Transaldolase Activity in the Isolated Heart Supplied with [U-$^{13}C_3$]Glycerol*

Received for publication, August 9, 2012, and in revised form, November 13, 2012 Published, JBC Papers in Press, December 12, 2012, DOI 10.1074/jbc.M112.409441

Eunsook S. Jin[‡§1], **A. Dean Sherry**[‡¶‖], **and Craig R. Malloy**[‡§¶**]

From the [‡]*Advanced Imaging Research Center,* [§]*Department of Internal Medicine, and* [¶]*Radiology, University of Texas Southwestern Medical Center, Dallas, Texas 75390, the* [‖]*Department of Chemistry, University of Texas at Dallas, Richardson, Texas 75080, and the* [**]*Veterans Affairs North Texas Health Care System, Dallas, Texas 75216*

Background: The metabolic fate of glycerol in the heart is controversial.
Results: [U-$^{13}C_3$]Glycerol is metabolized to glycogen, but the label is only found in carbon positions 4–6 of each glucose moiety.
Conclusion: This isotopomer pattern can only be ascribed to transaldolase activity.
Significance: This is the first detection of transaldolase activity of an isolated organ using a stable isotope.

Studies of glycerol metabolism in the heart have largely emphasized its role in triglyceride synthesis. However, glycerol may also be oxidized in the citric acid cycle, and glycogen synthesis from glycerol has been reported in the nonmammalian myocardium. The intent of this study was to test the hypothesis that glycerol may be metabolized to glycogen in mammalian heart. Isolated rat hearts were supplied with a mixture of substrates including glucose, lactate, pyruvate, octanoate, [U-$^{13}C_3$]glycerol, and ^2H_2O to probe various metabolic pathways including glycerol oxidation, glycolysis, the pentose phosphate pathway, and carbon sources of stored glycogen. NMR analysis confirmed that glycogen production from the level of the citric acid cycle did not occur and that the glycerol contribution to oxidation in the citric acid cycle was negligible in the presence of alternative substrates. Quite unexpectedly, ^{13}C from [U-$^{13}C_3$]glycerol appeared in glycogen in carbon positions 4–6 of glucosyl units but none in positions 1–3. The extent of [4,5,6-$^{13}C_3$]glucosyl unit enrichment in glycogen was enhanced by insulin but decreased by H_2O_2. Given that triose phosphate isomerase is generally assumed to fully equilibrate carbon tracers in the triose pool, the marked ^{13}C asymmetry in glycogen can only be attributed to conversion of [U-$^{13}C_3$]glycerol to [U-$^{13}C_3$]dihydroxyacetone phosphate and [U-$^{13}C_3$]glyceraldehyde 3-phosphate followed by rearrangements in the nonoxidative branch of the pentose phosphate pathway involving transaldolase that places this ^{13}C-enriched 3-carbon unit only in the bottom half of hexose phosphate molecules contributing to glycogen.

Free fatty acids, lactate and glucose are primary substrates for cardiac energy production, but the heart has the capacity to oxidize a wide variety of alternative compounds. In mammalian heart tissue, ^{14}C-enriched glycerol was readily oxidized to $^{14}CO_2$ even in the presence of glucose or long chain fatty acids (1, 2). Glycerol is phosphorylated by glycerol kinase to form glycerol 3-phosphate, and this intermediate is then converted to dihydroxyacetone phosphate (DHAP)[2] which is rearranged to D-glyceraldehyde 3-phosphate (GA3P) via triose phosphate isomerase (TPI; EC 5.3.1.1). GA3P may be further metabolized to pyruvate and enter the citric acid cycle via pyruvate dehydrogenase, or pyruvate may supply carbon to the cycle via pyruvate carboxylase without net oxidation (3). Another metabolic fate of glycerol after phosphorylation is that it is readily utilized in the synthesis of triglycerides and phospholipids in the mammalian heart (2). Although the heart is not a glyconeogenic organ, the enzymes necessary to convert glycerol to glucose 1-phosphate (G1P) and glycogen are all present, and conversion of ^{14}C-enriched glycerol to glycogen in isolated heart tissue of nonmammalian species has been reported (4). The quantitative significance of this conversion in mammalian tissue has not been examined.

The physiological range of glycerol in plasma is 0.04-0.4 mM (5–7), but it may be increased severalfold under the condition of starvation (7), exercise (8), exposure to cold (9), or diabetes (10). The combination of fasting and cold exposure increased plasma glycerol up to ~1 mM in rodents (9). Furthermore, athletes who drink beverages containing extra glycerol for improving exercise performance and hydration status may reach up to ~10 mM glycerol in plasma with the dose of 1 g/kg body weight (11, 12). In this study, [U-$^{13}C_3$]glycerol was supplied to isolated rat hearts with the intent of quantifying the contribution of glycerol to assess exchange of glycerol into the glucosyl carbons of glycogen. With full exchange at the level of TPI, labeling in the top and bottom of glucosyl units of glycogen should be equal whereas incomplete exchange in the triose pool should result in preferential enrichment of carbons 1–3 of glucosyl units in glycogen. Surprisingly, we found that [U-$^{13}C_3$]glycerol is transferred exclusively to carbons 4–6 of glucosyl units with

* This study was supported, in whole or in part, by National Institutes of Health Grants K01-DK078933 (to E. S. J.), RR-02584 (to C. R. M.), and HL-34557 (to A. D. S.).

[1] To whom correspondence should be addressed: Advanced Imaging Research Center, 5323 Harry Hines Blvd., Dallas, TX 75390-8568. Tel.: 214-645-2725; Fax: 214-645-2744; E-mail: eunsook.jin@utsouthwestern.edu.

[2] The abbreviations used are: DHAP, dihydroxyacetone phosphate; F6P, fructose 6-phosphate; GA3P, D-glyceraldehyde 3-phosphate; G1P, glucose 1-phosphate; G6P, glucose 6-phosphate; G6PD, glucose 6-phosphate dehydrogenase; ^2H_2O, deuterated water; KHB, Krebs-Henseleit bicarbonate; MAG, monoacetone glucose; 6PGD, 6-phosphogluconate dehydrogenase; PPP, pentose phosphate pathway; S7P, sedoheptulose 7-phosphate; TPI, triose phosphate isomerase.

no enrichment in carbons 1–3. This observation can only be explained by carbon rearrangements occurring at the level of transaldolase in the nonoxidative portion of the pentose phosphate pathway (PPP).

EXPERIMENTAL PROCEDURES

Materials—[U-$^{13}C_3$]Glycerol (99%), [1,2-$^{13}C_2$]glucose (99%), and ^2H_2O (99%) were obtained from Cambridge Isotope Laboratories, Inc. (Andover, MA). DL-Isoproterenol hydrochloride, cation-exchange (Dowex 50WX8-200) and anion-exchange (Amberlite IRA-67) resin, and other common chemicals were obtained from Sigma.

Isolated Heart Preparation—The protocol was approved by the Institutional Animal Care and Use Committee at the University of Texas Southwestern Medical Center. Under general anesthesia, hearts (1.5 ± 0.2 g) from overnight-fasted male Sprague-Dawley rats (300–350 g) were rapidly excised and perfused using standard Langendorff methods at 37 °C and 100-cm H_2O with a Krebs-Henseleit bicarbonate (KHB) buffer (3). The KHB buffer, bubbled continuously with a 95/5 mixture of O_2/CO_2, contained 25 mM $NaHCO_3$, 118 mM NaCl, 4.7 mM KCl, 1.2 mM $MgSO_4$, 1.2 mM KH_2PO_4, 0.5 mM EDTA (sodium salt), 2.5 mM $CaCl_2$, 1.2 mM lactate, and 0.12 mM pyruvate. The heart rate was monitored through an open-ended cannula in the left ventricle. In one set of studies, the heart was preperfused with 8 nM isoproterenol solution containing 0.5 mM octanoate, 1.2 mM lactate, and 0.12 mM pyruvate for 20 min to reduce glycogen content, followed by a 5-min perfusion with a mixture of the same substrates to wash out isoproterenol in the medium. In other studies, the heart was preperfused with a substrate-free KHB buffer without isoproterenol for 20 min to reduce glycogen. In all experiments the heart was perfused subsequently for 60 min with a medium containing 0.5 mM octanoate, 1.2 mM lactate, 0.12 mM pyruvate, 10 mM glucose, 2 mM glycerol, and 0.5% BSA to assure identical substrate conditions for all hearts. Depending on the experiment, deuterated water (^2H_2O), insulin, or hydrogen peroxide (H_2O_2) was added, or [U-$^{13}C_3$]glycerol or [1,2-$^{13}C_2$]glucose was substituted for the unlabeled compound, as follows: (i) 2 mM [U-$^{13}C_3$]glycerol and no insulin; (ii) 2 mM [U-$^{13}C_3$]glycerol and 50 microunits/ml insulin; (iii) 2 mM [U-$^{13}C_3$]glycerol, 50 microunits/ml insulin, and 0.1 mM H_2O_2; or (iv) 2 mM unlabeled glycerol, 10 mM [1,2-$^{13}C_2$]glucose, 50 microunits/ml insulin, and 5% ^2H_2O. After the perfusion, each heart was freeze clamped.

Preparation of Samples for NMR Analysis—Glycogen was extracted from frozen heart tissue using standard methods (13). Isolated glycogen was dissolved in 5 ml of 10 mM sodium acetate solution (pH 4.8) and incubated with amyloglucosidase (50 mg of glycogen/20 units of amyloglucosidase) for 4 h at 50 °C. After neutralizing, the hydrolyzed glycogen solution was applied to an ion exchange column containing 15 ml of the cation-exchange (Dowex 50WX8-200) and 15 ml of the anion-exchange (Amberlite IRA-67) resin. Hydrolyzed glycogen was purified by passage through the column using deionized water as eluent, collected, and lyophilized.

Glucosyl units from tissue glycogen were converted to monoacetone glucose (MAG) as follows. Dried glucose was suspended in 3.0 ml of acetone containing 120 μl of concentrated sulfuric acid. The mixture was stirred for 4 h at room temperature to yield diacetone glucose. After adding 3 ml of water, the pH was adjusted to 2.0 by dropwise addition of 1.5 M Na_2CO_3. The mixture was stirred for 24 h at room temperature to convert diacetone glucose into MAG. The pH was then further increased to ~8.0 by addition of Na_2CO_3. The acetone was evaporated under vacuum, and the sample was freeze-dried. MAG was extracted into 3 ml of hot ethyl acetate (5×), the solutions were combined, and ethyl acetate was removed by vacuum evaporation. The resulting MAG was further purified by passage through a 3-ml DSC-18 cartridge, using 5% acetonitrile as eluent. The effluent was freeze-dried and stored dry before NMR analysis.

A standard perchloric acid extraction procedure was used to extract water-soluble components from some hearts perfused with [U-$^{13}C_3$]glycerol for NMR analysis of the citric acid cycle intermediates and exchanging pools. In addition, effluent from the heart perfused with [1,2-$^{13}C_2$]glucose was treated with perchloric acid for NMR analysis of ^{13}C-enriched lactate.

NMR Spectroscopy—All NMR spectra were collected using a Varian Inova 14.1T spectrometer (Agilent, Santa Clara, CA) equipped using a 3-mm broadband probe with coil tunable to ^1H (600 MHz), ^2H (92 MHz), or ^{13}C (150 MHz). Hydrolyzed glycogen or perchloric acid extracts were dissolved in ^2H_2O (160 μl) for ^1H and ^{13}C NMR acquisition. ^1H NMR was acquired at 25 °C, using a 90° observe pulse, a 2-s acquisition time, and 1-s delay between pulses. The solvent water signal was presaturated using a frequency-selective pulse. Typically, 128 scans were summed requiring ~6 min. Proton-decoupled ^{13}C NMR spectra were acquired at 25 °C using a 45° pulse (5.0 μs), 34,965-Hz sweep width, 104,986 data points, and a 1.5-s interpulse delay at 25 °C. The samples were signal-averaged over 7,000–30,000 scans requiring 6–25 h. Proton decoupling was performed using a standard WALTZ-16 pulse sequence.

For ^2H NMR acquisition, MAG was dissolved in a mixture of 160 μl of acetonitrile and 10 μl of water. Proton-decoupled ^2H NMR spectra were acquired using a 90° pulse (12.5 μs), 920-Hz sweep width, 1,836 data points, and a 1-s acquisition time with no further delay at 50 °C. Typically ~70,000 scans were averaged, requiring ~21 h. After ^2H NMR acquisition, MAG was lyophilized and resuspended in 160 μl of deuterated acetonitrile (99.8%) and 10 μl of water for ^{13}C NMR acquisition. ^{13}C NMR spectra of MAG were collected using 52° pulse (6.06 μs), 20,330-Hz sweep width, 60,992 data points, and a 1.5-s acquisition time with 1.5-s interpulse delay at 25 °C. Typically ~25,000 scans were averaged, requiring ~25 h. All NMR spectra were analyzed using ACD/Labs PC-based NMR spectral analysis program (Advanced Chemistry Development, Inc., Toronto, ON, Canada).

Statistics—Data are expressed as means ± S.E. Comparisons between two groups were made using Student's two-tailed *t* test, where $p < 0.05$ was considered significant.

Pathway Considerations: ^{13}C Labeling of Glycogen in Hearts Supplied with [U-$^{13}C_3$]Glycerol—Given that the heart does not generate glycogen from the citric acid cycle, the only possible pathway for [U-$^{13}C_3$]glycerol to contribute to glucosyl units in glycogen must involve exchanges occurring at the level of TPI. In the "standard" gluconeogenesis in general, carbons 1–3 of

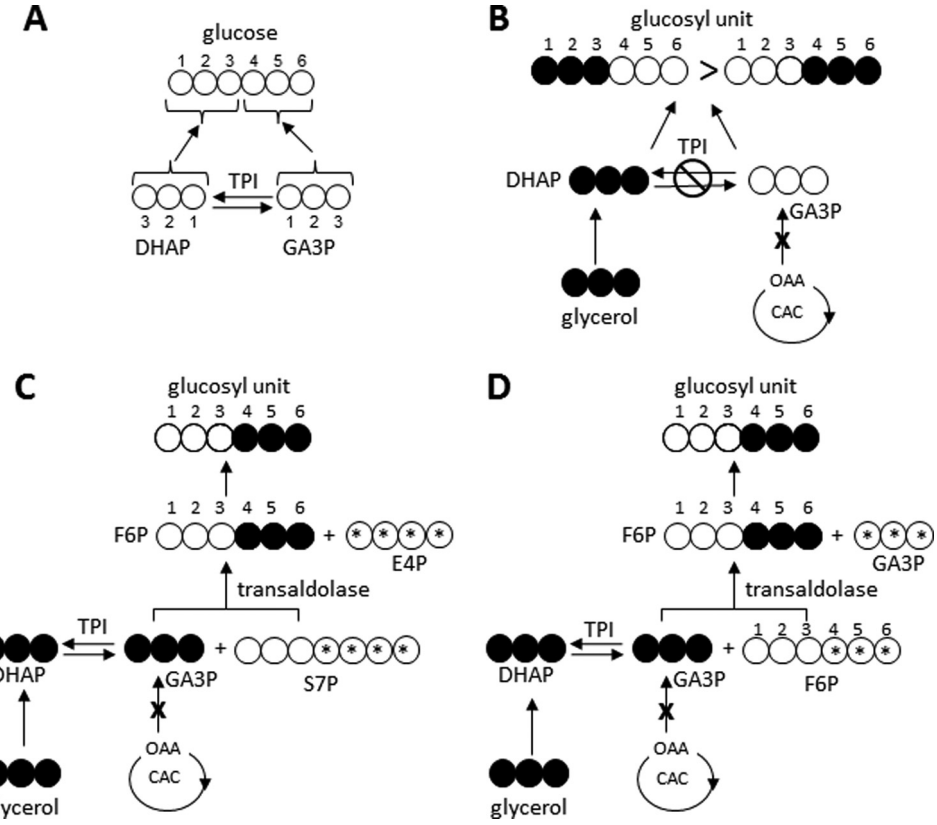

FIGURE 1. **Possible metabolic routes for unequal ^{13}C enrichment of carbons 1–3 *versus* 4–6 of glucosyl units of glycogen in heart supplied with [U-$^{13}C_3$]glycerol.** *A*, during glucose production through standard gluconeogenic pathways, carbons 1–3 of glucose originate from DHAP whereas carbons 4–6 originate from GA3P. *B*, in hearts exposed to [U-$^{13}C_3$]glycerol, one would anticipate that incomplete equilibration at the level of TPI would yield more [1,2,3-$^{13}C_3$]glucosyl units than [4,5,6-$^{13}C_3$]glucosyl units because [U-$^{13}C_3$]glycerol is converted first to [U-$^{13}C_3$]DHAP before [U-$^{13}C_3$]GA3P is produced at the level of TPI. *C*, in comparison, rapid equilibration of [U-$^{13}C_3$]GA3P with S7P at the level of transaldolase would yield only [4,5,6-$^{13}C_3$]F6P and E4P. *D*, transaldolase exchange between carbons 4–6 of F6P and [U-$^{13}C_3$]GA3P would also yield only [4,5,6-$^{13}C_3$]F6P. *OAA*, oxaloacetate; *E4P*, erythrose 4-phosphate; *CAC*, citric acid cycle; *open circles*, ^{12}C; *filled circles*, ^{13}C. The *x* indicates that flow of ^{13}C from the citric acid cycle into glycogen production is not considered in these examples. The *asterisks* in *C* and *D* indicate the carbons that are replaced by [U-$^{13}C_3$]GA3P through transaldolase activity to form [4,5,6-$^{13}C_3$]F6P.

glucose (the "top half") are derived from DHAP whereas carbons 4–6 (the "bottom half") are derived from GA3P (Fig. 1*A*) and, because phosphorylation of [U-$^{13}C_3$]glycerol would form [U-$^{13}C_3$]DHAP in two steps if complete equilibration at the level of TPI does not occur, this should produce more [1,2,3-$^{13}C_3$]glucosyl units (the DHAP end) than [4,5,6-$^{13}C_3$]glucosyl units (the GA3P end; Fig. 1*B*). If the trioses fully equilibrate at the level of TPI and this is the only pathway leading to glucosyl units, the labeling of the top and bottom ends of glucosyl units must be identical. On the other hand, if other exchanges occur rapidly in the nonoxidative portion of the PPP, then the labeling pattern could be quite different. For example, transaldolase (EC 2.2.1.2) catalyzes removal of a 3-carbon dihydroxyacetone unit from the nonphosphorylated end of sedoheptulose 7-phosphate (S7P), and this 3-carbon unit can then condense with any [U-$^{13}C_3$]GA3P that might be present to yield [4,5,6-$^{13}C_3$]-fructose 6-phosphate (F6P) and erythrose 4-phosphate (Fig. 1*C*). This [4,5,6-$^{13}C_3$]F6P would be readily converted to [4,5,6-$^{13}C_3$]glucose 6-phosphate (G6P) and subsequently [4,5,6-$^{13}C_3$]G1P and glycogen with glucosyl units labeled only in the 4,5,6 positions.

Transaldolase Exchange—Ljungdahl *et al.* (14) demonstrated that isolated transaldolase can exchange carbons 4–6 of F6P with GA3P even in the absence of other enzymes or intermediates of the PPP. If this exchange between F6P and [U-$^{13}C_3$]GA3P should occur in heart, this would also result in exclusive labeling of the 4–6 carbons of glucosyl units of glycogen (Fig. 1*D*).

RESULTS

Hearts Supplied with [U-$^{13}C_3$]Glycerol—A ^{13}C NMR spectrum of MAG derived from hydrolyzed glycogen is shown in Fig. 2. Clearly, excess ^{13}C was evident only in carbons 4, 5, and 6 of glucosyl units of glycogen in hearts supplied with [U-$^{13}C_3$]glycerol and other natural abundance substrates. Preferential labeling of the bottom half could in principle arise from metabolism of [U-$^{13}C_3$]glycerol in the citric acid cycle followed by conversion of ^{13}C-enriched citric acid cycle intermediates to phospho*enol*pyruvate and ultimately GA3P, but this is highly unlikely because only intact, three-carbon ^{13}C-enriched units were found in glycogen as [4,5,6-$^{13}C_3$]glucose moiety.

Although glycogen synthesis from the citric acid cycle is not considered active in the heart, we reexamined the possibility that [U-$^{13}C_3$]glycerol under these conditions could be metabolized to pyruvate followed by oxidation to acetyl-CoA or carboxylation to oxaloacetate. The presence of [U-$^{13}C_3$]lactate resonances in the ^{13}C NMR spectra of heart tissue extracts demonstrated that the glycerol was indeed metabolized to

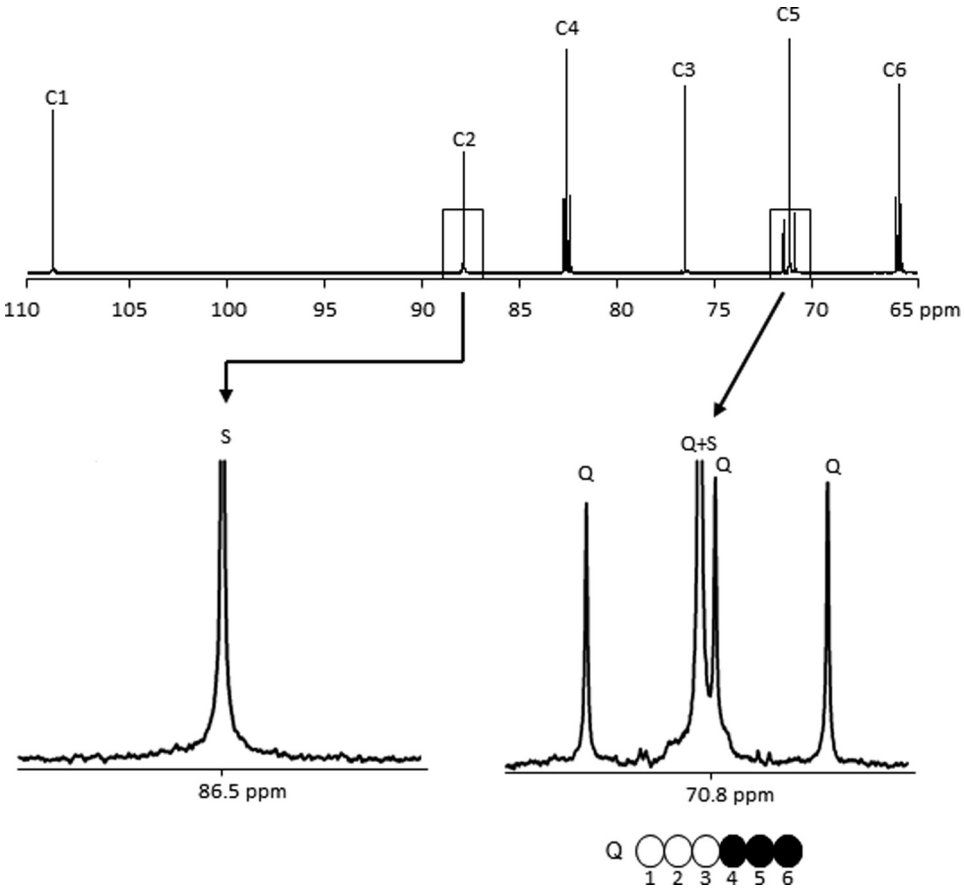

FIGURE 2. **^{13}C NMR spectrum of MAG derived from hydrolyzed glycogen of a heart supplied with [U-$^{13}C_3$]glycerol.** The multiplets seen in the C4, C5, and C6 resonances but not in the C1, C2, and C3 resonances indicate that carbons originating in [U-$^{13}C_3$]glycerol find their way only into the bottom half of glucosyl units of glycogen. The singlets detected in each glucosyl unit resonance reflect largely natural abundance levels of ^{13}C. *Q*, doublet of doublets, or quartet, arising from coupling of C5 with both C4 and C6; *S*, singlet.

pyruvate (Fig. 3). However, the ^{13}C signals in glutamate were almost exclusively at natural abundance levels except the very small amount of [4,5-$^{13}C_2$]glutamate (0.022 ± 0.006%, $n = 5$). This labeling at C4–C5 of glutamate demonstrated that [U-$^{13}C_3$]glycerol did indeed enter the citric acid cycle as acetyl-CoA, but the fraction of acetyl-CoA derived from glycerol was <1%. Pyruvate carboxylation to oxaloacetate was not detected as evidenced by the absence of excess ^{13}C enrichment in glutamate C1–C3. Clearly, small amount of [4,5-$^{13}C_2$]glutamate formed in the cycle could not have contributed significantly to the [4,5,6-$^{13}C_3$]glucose moiety in glycogen.

The labeling pattern in glycogen cannot be explained by simple condensation of GA3P and DHAP at the level of TPI. Incomplete equilibration of 3-carbon units at TPI would result in excess enrichment in the top half of glucosyl units, *i.e.* [1,2,3-$^{13}C_3$]glucose (Fig. 1*B*). The appearance of [4,5,6-$^{13}C_3$]glucosyl units alone, however, must reflect some combination of transaldolase activity between [U-$^{13}C_3$]GA3P and S7P (Fig. 1*C*), and transaldolase exchange between the bottom half carbons of F6P and [U-$^{13}C_3$]GA3P (Fig. 1*D*). The ^{13}C enrichment in cardiac glycogen was measured using ^{13}C NMR analysis of α- and β-glucose *C*6 resonances after the hydrolysis of glycogen, assuming that the singlet peaks seen in the C6 resonances represent natural abundance ^{13}C. The areas of the multiplets in the C6 resonances indicated that [U-$^{13}C_3$]glycerol contributed to ~0.51% and ~1.21% of the total glucose derived from tissue glycogen in the absence and presence of insulin, respectively (Fig. 4, *A* and *B*). Thus, insulin enhanced ^{13}C enrichment in glycogen approximately 2-fold whereas it did not affect glycogen content (Fig. 4*C*).

The unexpected labeling pattern in glycogen remained the same whether hearts were preperfused with isoproterenol or with a substrate-free KHB buffer, confirming that the asymmetry was not related to a residual effect of isoproterenol (Fig. 4). The enrichment of [4,5,6-$^{13}C_3$]glucosyl units from the hearts preperfused with a buffer was not different statistically from the hearts pretreated with isoproterenol (Fig. 4, *A* and *B*). In contrast, adding H_2O_2 in the hearts preperfused with a buffer decreased the enrichment compared with the hearts pretreated with isoproterenol. However, glycogen content was not affected by insulin, H_2O_2, or pretreatment with isoproterenol (Fig. 4*C*). All of the hearts under the various conditions were functioning well as evidenced by heart beating rates and oxygen consumption (Table 1).

Hearts Supplied with [1,2-$^{13}C_2$]Glucose and ^2H_2O—To determine whether the observed asymmetry required flux of exogenous glucose into the triose phosphate pool, a second group of hearts were supplied with medium containing [1,2-$^{13}C_2$]glucose and 5% ^2H_2O in addition to unlabeled glycerol. The ^{2}H NMR spectrum of MAG derived from glycogen showed

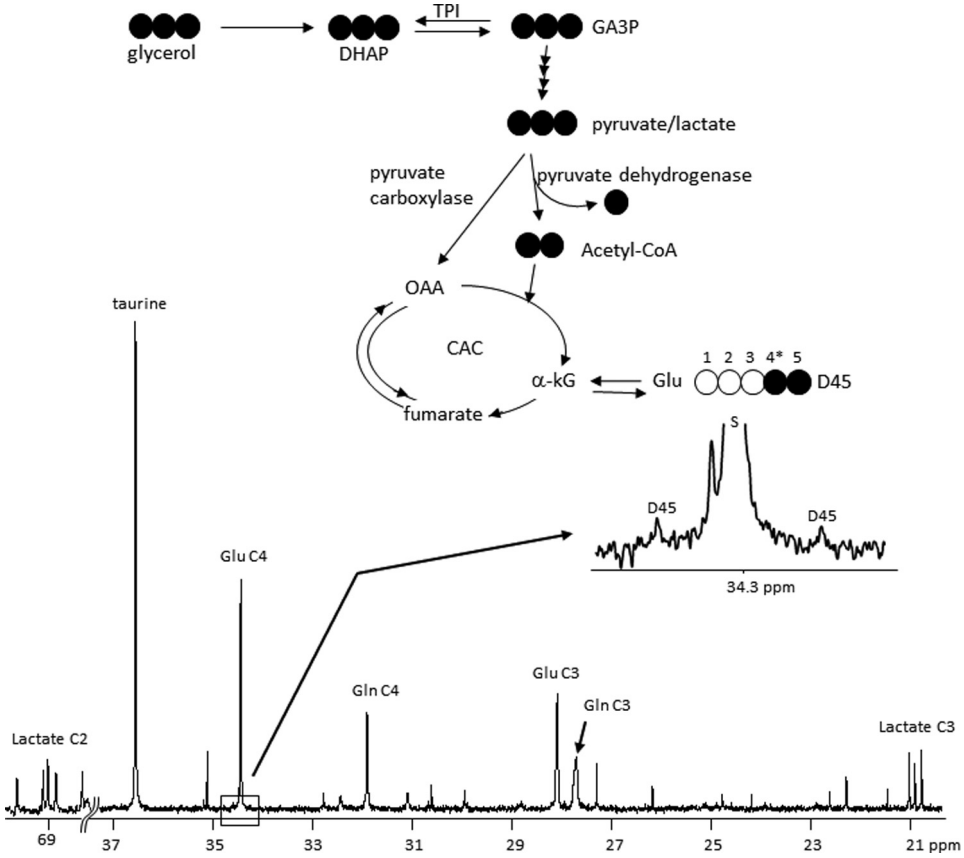

FIGURE 3. **^{13}C NMR spectrum of a heart tissue extract after perfusion with [U-$^{13}C_3$]glycerol.** Only natural-abundance singlets were detected in glutamate, glutamine, and taurine, with the exception that [4,5-$^{13}C_2$]glutamate was observed at a very low level (0.022 ± 0.006%, $n = 5$). Resonance of glutamate C4 is expanded. The multiplets in lactate resonances are from [U-$^{13}C_3$]lactate, which is in exchange with [U-$^{13}C_3$]pyruvate in tissues. Because glutamate is in rapid exchange with α-ketoglutarate (*α-kG*), the presence of the small doublets due to ^{13}C-^{13}C spin-spin coupling between C4 and C5 (*D45*) indicates that a small portion of [U-$^{13}C_3$]pyruvate entered the citric acid cycle through acetyl-CoA. *D45*, doublet arising from coupling of C4 with C5; *S*, singlet.

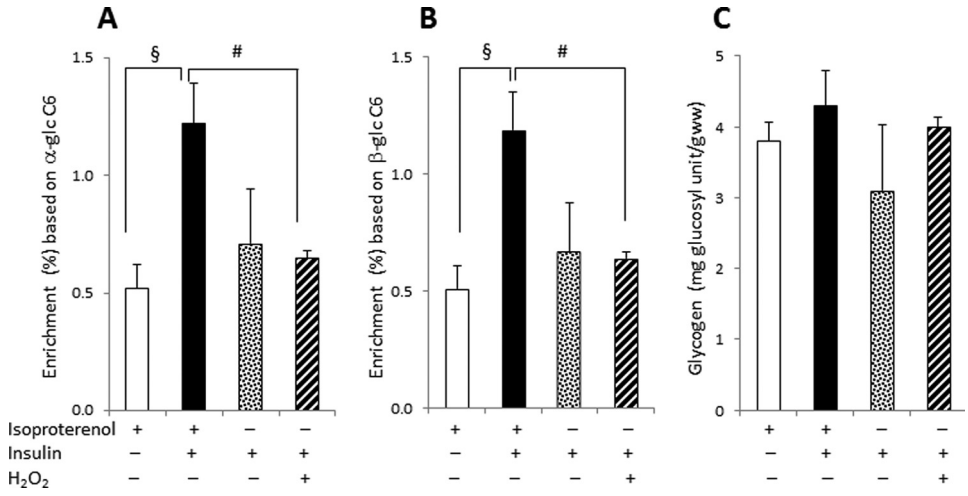

FIGURE 4. **Effect of isoproterenol pretreatment, insulin, or H_2O_2 on ^{13}C enrichment and total glycogen content in hearts supplied with [U-$^{13}C_3$]glycerol.** *A* and *B*, insulin increased the enrichment in the [4,5,6-$^{13}C_3$]glucosyl units of glycogen based on the ^{13}C NMR analysis of hydrolyzed α-glucose C6 (*A*) and β-glucose C6 (*B*), but H_2O_2 decreased the enrichment. *C*, glycogen content remained the same by the presence of insulin or H_2O_2. Glycogen content was not different in hearts preperfused with isoproterenol compared with preperfusion with a substrate-free buffer without isoproterenol. *glc* C6, carbon 6 of glucosyl unit; #, $p < 0.05$; §, $p < 0.01$.

~0.5–0.6% ^{2}H enrichment in H1 and H2 positions, ~0.07–0.08% enrichment in H4 and H5, but no excess enrichment in other proton positions (Fig. 5). ^{2}H enrichment at the H1 and H2 positions was the result of exchange reactions occurring at the level of hexose phosphates, whereas ^{2}H enrichment at H4 and H5 originate from exchange reactions occurring at the level of triose phosphates. The absence of enrichment at H3 informed that DHAP did not contribute to carbons 1–3 of glucosyl units of glycogen through the standard glyconeogenic pathways from the triose pool because ^{2}H incorporation at H3 position also

TABLE 1

Heart rates and O_2 consumption

Hearts were preperfused with isoproterenol solution for 20 min or with a substrate-free buffer without isoproterenol for 20 min to reduce glycogen content. A 60-min perfusion followed with media containing octanoate, lactate, pyruvate, glucose, and [U-$^{13}C_3$]glycerol. Insulin and/or H_2O_2 were added in some cases, which are specified below.

Pre-perfusion with isoproterenol & perfusion without insulin (n=5-6)

heart rate (beats/min)			O_2 consumption (μmol/gww/min)		
isoproterenol	+20 min	+40 min	isoproterenol	+20 min	+40 min
268 ± 14[§]	184 ± 21	180 ± 23	2.6 ± 0.3	2.8 ± 0.3	3.0 ± 0.2

Pre-perfusion with isoproterenol & perfusion with insulin (n=8-10)

heart rate (beats/min)			O_2 consumption (μmol/gww/min)		
isoproterenol	+20 min	+40 min	isoproterenol	+20 min	+40 min
323 ± 16[¥]	225 ± 14	232 ± 15	4.0 ± 0.7	3.1 ± 0.4	3.0 ± 0.4

Pre-perfusion with a buffer & perfusion with insulin (n=4)

heart rate (beats/min)			O_2 consumption (μmol/gww/min)		
buffer only	+20 min	+40 min	buffer only	+20 min	+40 min
335 ± 9	313 ± 21	318 ± 24	4.3 ± 0.4	4.2 ± 0.5	4.2 ± 0.4

Pre-perfusion with a buffer & perfusion with insulin and H_2O_2 (n=4)

heart rate (beats/min)			O_2 consumption (μmol/gww/min)		
buffer only	+20 min	+40 min	buffer only	+20 min	+40 min
338 ± 10	278 ± 11	293 ± 11	4.1 ± 0.2	4.5 ± 0.2	4.2 ± 0.3

[§], $p \leq 0.01$; [¥], $p < 0.001$ compared with the time point at either +20 min or +40 min.

occurs at the level of TPI (DHAP ← GA3P) (15). Otherwise, the enrichment at H3 of glucosyl units would be observed, which originates from H1 position of DHAP. The absence of enrichment at H6 confirmed that the citric acid cycle did not contribute to glycogen because ^{2}H incorporation at H6 occurs at the level of fumarase (16). The dominant ^{2}H enrichment at the H1 and H2 positions of [1,2-$^{13}C_2$]glucose units from glycogen (Fig. 5) informed that newly synthesized glycogen was mainly from exogenous glucose incorporation. The ^{13}C NMR spectra confirmed that the overwhelming majority of glycogen was produced by direct phosphorylation of [1,2-$^{13}C_2$]glucose into glycogen rather than breakdown to the level of trioses followed by synthesis to glycogen (spectra not shown).

The fraction of newly synthesized glycogen that occurred during the perfusion period was determined by ^{1}H NMR analysis of hydrolyzed glycogen (Fig. 6*A*). Fig. 6*A* shows the ^{1}H NMR spectrum of glucose derived from glycogen with the H1 resonance showing the ^{13}C satellite peaks characteristic of enrichment in carbon 1. Because the proton signals in positions 1 and 2 are both split due to J_{CH} scalar coupling, the fraction of glycogen from perfusate [1,2-$^{13}C_2$]glucose is simply the area of the doublet relative to total signal. In this case, 23 ± 1% (n = 6) of total glycogen was derived from [1,2-$^{13}C_2$]glucose. This demonstrates that pretreatment with isoproterenol did not deplete the entire glycogen pool.

Lactate in the effluent was also examined by ^{13}C NMR. Glycolysis of [1,2-$^{13}C_2$]glucose will produce [2,3-$^{13}C_2$]lactate whereas any flux through the oxidative portion of the PPP would yield [3-$^{13}C_1$]lactate. The spectra shown in Fig. 6*B* provide direct evidence that no [3-$^{13}C_1$]lactate was formed as a result of glucose passing through the PPP. Here, the singlet components seen in the C2 and C3 resonances of lactate have identical intensities so must reflect only natural abundance levels of ^{13}C. This demonstrates that the oxidative portion of the PPP was not active in these hearts.

DISCUSSION

The observation that carbons from [U-$^{13}C_3$]glycerol appear exclusively in the 4,5,6-positions of glucosyl units of newly formed glycogen in hearts perfused with a mixture of substrates confirms earlier observations that glycerol can indeed supply carbons to glycogen in the nonmammalian heart (4). The lack of ^{13}C enrichment in the carbons 1, 2, or 3 demonstrates that conversion of glycerol to glycogen does not occur via the standard glyconeogenic pathways (DHAP + GA3P → Fru-1,6-P_2 → F6P → G6P → G1P → glycogen) but rather must involve rearrangements in the nonoxidative portion of the PPP. The rather dramatic ^{13}C asymmetry found in glycogen (Fig. 2) was quite surprising. The data shown here by ^{13}C NMR isotopomer analysis of tissue glutamate showed that very little [U-$^{13}C_3$]glycerol (<1%) contributes to acetyl-CoA in the citric acid cycle even though [U-$^{13}C_3$]lactate is formed. Furthermore, ^{2}H NMR of MAG derived from tissue glycogen in hearts exposed to ^2H_2O indicates that, within error of the measurement, none of the glucosyl units in glycogen comes from the level of the citric acid cycle (Fig. 5), as expected for this nonglyconeogenic tissue. Thus, the only reasonable explanation for the observations seen here must involve carbon rearrangements in the PPP catalyzed by transaldolase.

The PPP is described as having two components, the oxidative segment that produces NADPH and ribulose 5-phosphate from 6-phosphogluconate and the nonoxidative segment that

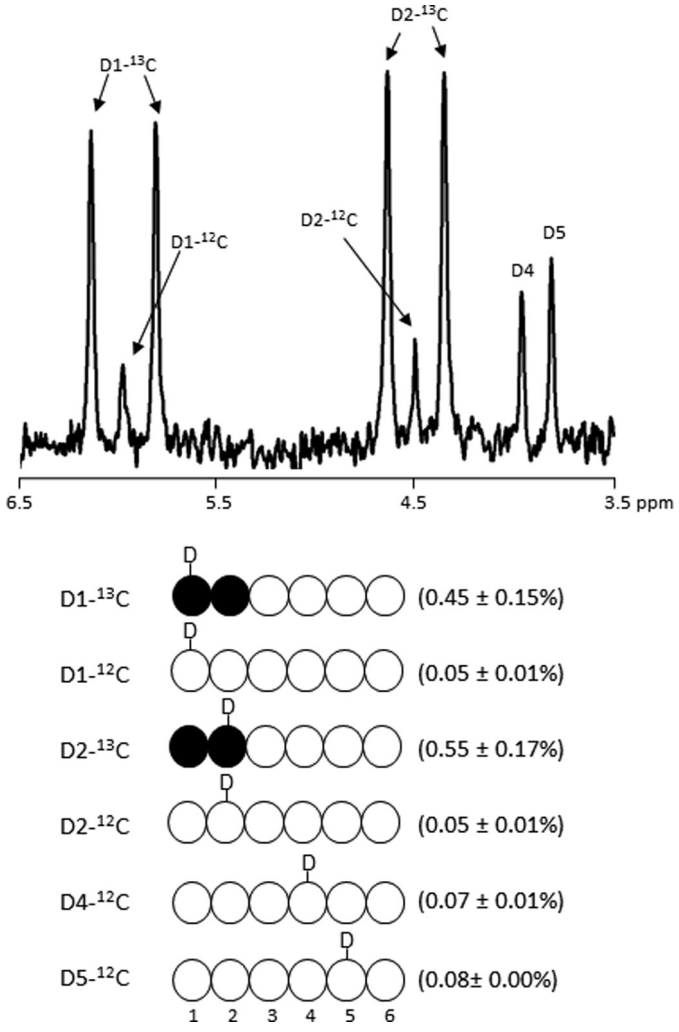

FIGURE 5. **^2H NMR spectrum of MAG derived from glycogen isolated from a heart supplied with [1,2-$^{13}C_2$]glucose and ^2H_2O.** In the presence of ^2H_2O, deuterium (^2H or D) enrichment is found in positions H1, H2, H4, and H5, but not in H3, $H6_R$, and $H6_S$. The absence of enrichment at H3 informs that DHAP did not contribute to carbons 1–3 of glucosyl units of glycogen through the standard glyconeogenic pathways (DHAP + GA3P → Fru-1,6-P_2 → F6P → G6P → G1P → glycogen). The absence of ^2H enrichment at the H6 position demonstrates the absence of glyconeogenesis from the citric acid cycle. The enrichment values shown in parentheses are average ± S.E. (n = 3). *D1*, *D2*, etc. indicate deuterium at glucosyl unit C1 position, C2 position, etc.

interconverts sugar phosphates formed in glycolysis with the pentose phosphates. Transaldolase catalyzes exchange of 3-carbon sugar units, with the most widely accepted reaction being interconversion of GA3P and S7P to form erythrose 4-phosphate and F6P. However, it has also been reported that isolated transaldolase can directly exchange the carbons 4,5,6 of F6P with GA3P even in the absence of other enzymes or intermediates of the PPP (14). Transaldolase is active in the heart, although at a lower level compared with the kidney or liver (17, 18). The fact that the fraction of glycogen derived through the transaldolase reaction increased in the presence of insulin suggests that flux through this pathway may be physiologically significant. However, at least in normal myocardium the fraction of glycogen labeled with ^{13}C from [U-$^{13}C_3$]glycerol was small, on the order of 5–6%, compared with the glycogen derived directly from exogenous glucose. Nevertheless, the fact that genetic defects in transaldolase have been associated with cardiomyopathy (19) suggests that transaldolase may play a significant role under some pathophysiological conditions.

Transaldolase was also reported to play a key role in redox homeostasis (20, 21), and oxidative damage is involved in many diseases including heart failure (22–24). The decreased [U-$^{13}C_3$]glycerol incorporation to glycogen via transaldolase in the presence of H_2O_2 (0.1 mM) supports the idea that it may play a role in regulation of redox. Reduced transaldolase activity was reported to correlate with increased activities of glucose-6-phosphate dehydrogenase (G6PD) and 6-phosphogluconate dehydrogenase (6PGD), and to increased level of reduced glutathione (GSH) in Jurkat human leukemic T cells (20). GSH is the primary antioxidant in most cells involved in reducing H_2O_2 to water (H_2O). The NADPH supply from the oxidative segment of the PPP is essential in maintaining GSH, and it is produced at the levels of G6PD and 6PGD. However, the precise mechanism remains to be investigated as to how transaldolase plays a role in antioxidant defense along with the enzymes of the oxidative segment. We also perfused hearts with a higher concentration of H_2O_2 (0.225 mM), which reduced the enrichment of [4,5,6-$^{13}C_3$]glucosyl units dramatically by ~10-fold, but the hearts functioned poorly, and the perfusions were discontinued before the planned 60-min duration (data not shown).

Although the pathophysiological relevance of transaldolase in heart is not well understood, its activity in the intact liver has been examined in some detail in part because it may result in overestimation of gluconeogenic flux using the ^2H_2O method introduced by Landau and his co-workers (25–28). The distribution of ^2H in glucose, after the administration of ^2H_2O, is commonly used to measure the relative activity of gluconeogenesis and glycogenolysis in hepatic glucose production. In principle, ^2H labeling should occur in three-carbon units derived from either glycerol or the citric acid cycle at the level of TPI. The hydrogen destined to become the H5 of glucose exchanges with any ^2H in tissue water and thus reports the fraction of glucose derived from the sum of glycerol plus the citric acid cycle contribution, assuming equilibration in the TPI reaction. However, ^2H labeling of glucose H5 through transaldolase exchange was reported to result in overestimation of gluconeogenesis (26). The distribution of ^{13}C in urinary glucuronides was also reported to be sensitive to activity of liver transaldolase (28).

Flux through the PPP in heart is controversial in part because of difficulties related to the interpretation of $^{14}CO_2$ release from [1-^{14}C]glucose compared with $^{14}CO_2$ release from [6-^{14}C]glucose (29). Pfeiffer *et al.* concluded that PPP flux does not contribute significantly to NADPH production in the heart (30). However, Burns and Reddy found significant PPP flux in isolated cardiomyocytes (31). The current results provided no information about flux through the oxidative portion of the cycle but did illustrate the high activity of flux through the non-oxidative portion of the cycle.

After exposure of hearts to ^2H_2O, the absence of excess ^2H in glucose H6 demonstrated that none of the trioses involved with glucose production passed through the citric acid cycle. The enrichment of H4 and H5 occurred through ^2H incorporation

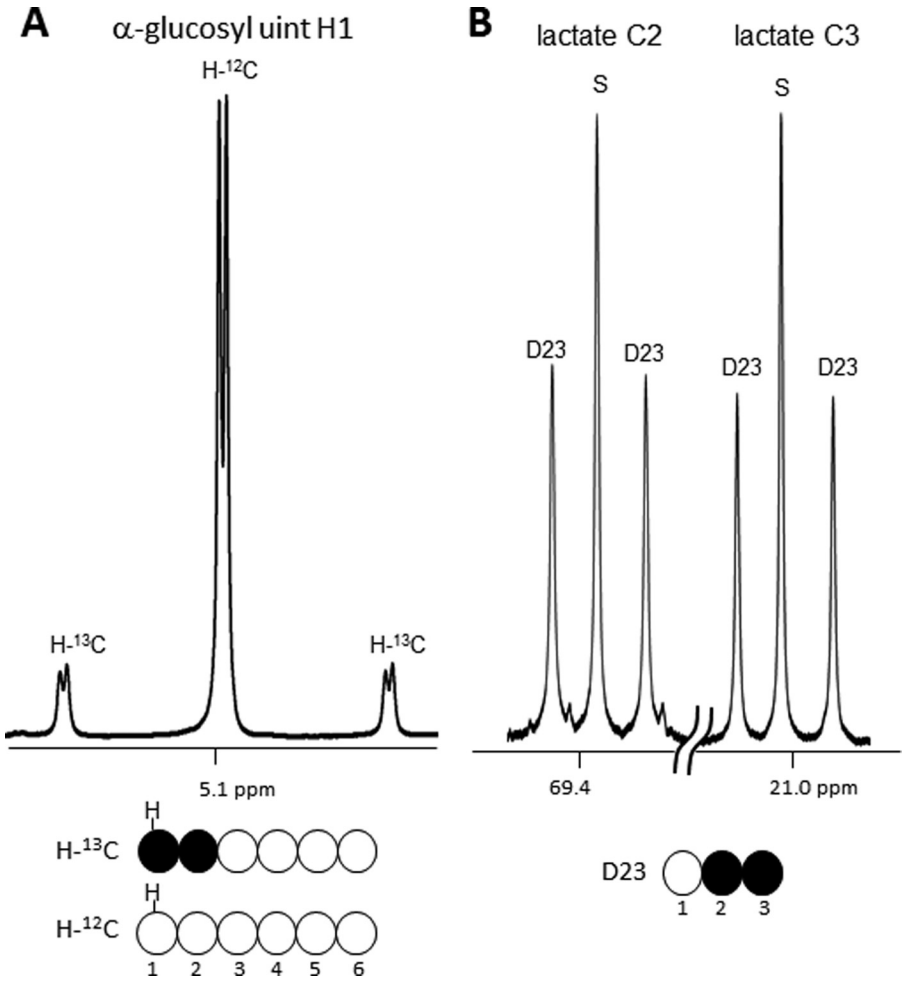

FIGURE 6. **^{1}H NMR and ^{13}C NMR spectra from a heart supplied with [1,2-$^{13}C_2$]glucose and $^{2}H_2O$.** *A*, ^{1}H NMR spectrum of hydrolyzed glycogen (H1 region of α-glucosyl units) from an isolated heart. The doublet due to scalar carbon-proton coupling in C1 of α-glucosyl units indicates that 23% of the glycogen was synthesized by direct phosphorylation of [1,2-$^{13}C_2$]glucose. *B*, glycolysis of [1,2-$^{13}C_2$]glucose produces [2,3-$^{13}C_2$]lactate. In contrast, flux through the oxidative arm of the PPP results in loss of carbon 1 with subsequent generation of [3-$^{13}C_1$]lactate. The singlet components in lactate C2 and C3 were essentially identical so must be assigned to natural abundance lactate. This shows that there was no significant flux of [1,2-$^{13}C_2$]glucose through the oxidative portion of the PPP. *D23*, doublet arising from coupling of C2 with C3; *S*, singlet due to natural abundance.

at the levels of triose phosphates. The absence of enrichment at H3 informed that carbons 1–3 of glucosyl units of glycogen were not originated directly from DHAP through the standard glyconeogenic pathways, in which the hydrogen destined to become the H3 of glucosyl units exchanges with ^{2}H in tissue water also occurs at the levels of triose phosphates, precisely originating from the H1 position of DHAP. The highest enrichment in H2 position of glucosyl units was due to ^{2}H incorporation at the level of G6P ↔ F6P exchange. The H1 position was also substantially labeled by ^{2}H, as observed previously in skeletal muscle glycogen (32). ^{2}H labeling at H1 can occur by two processes. First, ^{2}H incorporation at the level of mannose 6-phosphate isomerase (F6P ↔ mannose 6-phosphate) can lead to ^{2}H enrichment of H1 position of glucose (33). The other possibility is intramolecular exchange of ^{1}H in position 1 of F6P with ^{2}H in position 2 of G6P (34).

In contrast to earlier reports (1–2), we found that oxidation of glycerol in the citric acid cycle did not contribute significantly to energy production using a perfusion medium containing physiological amounts of other unlabeled substrates. As noted previously (35, 36), oxidation of any particular substrate is very sensitive to the concentrations of alternative substrates. Consequently, differing results are almost certainly due to differences in the availability of other oxidizable substrates. In the current study, octanoate likely suppressed glycerol oxidation and enabled detection of asymmetric labeling in glycogen.

In summary, ^{13}C labeling in carbons 4,5,6 of glucosyl units of glycogen in the heart after administration of [U-$^{13}C_3$]glycerol reflects flux through the following pathway: [U-$^{13}C_3$]glycerol → → [U-$^{13}C_3$]DHAP → [U-$^{13}C_3$]GA3P → [4,5,6-$^{13}C_3$]F6P → → [4,5,6-$^{13}C_3$]glucosyl units of glycogen. This observation is of interest in part because detection of transaldolase reactions may be important under conditions of oxidative stress.

Acknowledgments—We thank Charles Storey, Angela Milde, and Nicholas Carpenter for excellent technical help in the perfusion experiments.

REFERENCES

1. Gambert, S., Héliès-Toussaint, C., and Grynberg, A. (2005) Regulation of intermediary metabolism in rat cardiac myocyte by extracellular glycerol. *Biochim. Biophys. Acta* **1736,** 152–162

2. Gambert, S., Héliès-Toussaint, C., and Grynberg A. (2007) Extracellular glycerol regulates the cardiac energy balance in a working rat heart model. *Am. J. Physiol. Heart Circ. Physiol.* **292,** H1600–1606
3. Malloy, C. R., Sherry, A. D., and Jeffrey, F. M. (1988) Evaluation of carbon flux and substrate selection through alternate pathways involving the citric acid cycle of the heart by ^{13}C NMR spectroscopy. *J. Biol. Chem.* **263,** 6964–6971
4. Savina, M. V., and Wojtczak, A. B. (1977) Enzymes of gluconeogenesis and the synthesis of glycogen from glycerol in various organs of the lamprey (*Lampetra fluviatilis*). *Comp. Biochem. Physiol. B* **57,** 185–190
5. Lin, E. C. (1977) Glycerol utilization and its regulation in mammals. *Annu. Rev. Biochem.* **46,** 765–795
6. Rémésy, C., and Demigné, C. (1983) Changes in availability of glucogenic and ketogenic substrates and liver metabolism in fed or starved rats. *Ann. Nutr. Metab.* **27,** 57–70
7. Robinson, J., and Newsholme, E. A. (1969) The effects of dietary conditions and glycerol concentration on glycerol uptake by rat liver and kidney-cortex slices. *Biochem. J.* **112,** 449–453
8. Davis, S. N., Galassetti, P., Wasserman, D. H., and Tate, D. (2000) Effects of gender on neuroendocrine and metabolic counterregulatory responses to exercise in normal man. *J. Clin. Endocrinol. Metab.* **85,** 224–230
9. Brito, N. A., Brito, M. N., and Bartness, T. J. (2008) Differential sympathetic drive to adipose tissues after food deprivation, cold exposure or glucoprivation. *Am. J. Physiol. Regul. Integr. Comp. Physiol.* **294,** R1445–1452
10. van der Merwe, M. T., Schlaphoff, G. P., Crowther, N. J., Boyd, I. H., Gray, I. P., Joffe, B. I., and Lönnroth, P. N. (2001) Lactate and glycerol release from adipose tissue in lean, obese, and diabetic women from South Africa. *J. Clin. Endocrinol. Metab.* **86,** 3296–3303
11. van Rosendal, S. P., Osborne, M. A., Fassett, R. G., and Coombes, J. S. (2009) Physiological and performance effects of glycerol hyperhydration and rehydration. *Nutr. Rev.* **67,** 690–705
12. Massicotte, D., Scotto, A., Péronnet, F., M'Kaouar, H., Milot, M., and Lavoie, C. (2006) Metabolic fate of a large amount of ^{13}C-glycerol ingested during prolonged exercise. *Eur. J. Appl. Physiol.* **96,** 322–329
13. Jin, E. S., Burgess, S. C., Merritt, M. E., Sherry, A. D., and Malloy, C. R. (2005) Differing mechanisms of hepatic glucose overproduction in triiodothyronine-treated rats *vs*. Zucker diabetic fatty rats by NMR analysis of plasma glucose. *Am. J. Physiol. Endocrinol. Metab.* **288,** E654–662
14. Ljungdahl, L., Wood, H. G., Racker, E., and Couri, D. (1961) Formation of unequally labeled fructose 6-phosphate by an exchange reaction catalyzed by transaldolase. *J. Biol. Chem.* **236,** 1622–1625
15. Jones, J. G., Carvalho, R. A., Sherry, A. D., and Malloy, C. R. (2000) Quantitation of gluconeogenesis by ^{2}H nuclear magnetic resonance analysis of plasma glucose following ingestion of $^{2}H_2O$. *Anal. Biochem.* **277,** 121–126
16. Jones, J. G., Solomon, M. A., Cole, S. M., Sherry, A. D., and Malloy, C. R. (2001) An integrated ^{2}H and ^{13}C NMR study of gluconeogenesis and TCA cycle flux in humans. *Am. J. Physiol. Endocrinol. Metab.* **281,** E848–856
17. Heinrich, P. C., Morris, H. P., and Weber, G. (1976) Behavior of transaldolase (EC 2.2.1.2) and transketolase (EC 2.2.1.1) activities in normal, neoplastic, differentiating, and regenerating liver. *Cancer Res.* **36,** 3189–3197
18. James, H. M., Williams, S. G., Bais, R., Rofe, A. M., Edwards, J. B., and Conyers, R. A. (1985) The metabolic production of oxalate from xylitol: activities of transketolase, transaldolase, fructokinase and aldolase in liver, kidney, brain, heart, and muscle in the rat, mouse, guinea pig, rabbit and human. *Int. J. Vitam. Nutr. Res. Suppl.* **28,** 29–46
19. Verhoeven, N. M., Wallot, M., Huck, J. H., Dirsch, O., Ballauf, A., Neudorf, U., Salomons, G. S., van der Knaap, M. S., Voit, T., and Jakobs, C. (2005) A newborn with severe liver failure, cardiomyopathy and transaldolase deficiency. *J. Inherit. Metab. Dis.* **28,** 169–179
20. Banki, K., Hutter, E., Colombo, E., Gonchoroff, N. J., and Perl, A. (1996) Glutathione levels and sensitivity to apoptosis are regulated by changes in transaldolase expression. *J. Biol. Chem.* **271,** 32994–33001
21. Perl, A., Hanczko, R., Telarico, T., Oaks, Z., and Landas, S. (2011) Oxidative stress, inflammation and carcinogenesis are controlled through the pentose phosphate pathway by transaldolase. *Trends. Mol. Med.* **17,** 395–403
22. Belch, J. J., Bridges, A. B., Scott, N., and Chopra, M. (1991) Oxygen free radicals and congestive heart failure. *Br. Heart J.* **65,** 245–248
23. Hill, M. F., and Singal, P. K. (1996) Antioxidant and oxidative stress changes during heart failure subsequent to myocardial infarction in rats. *Am. J. Pathol.* **148,** 291–300
24. Mallat, Z., Philip, I., Lebret, M., Chatel, D., Maclouf, J., and Tedgui, A. (1998) Elevated levels of 8-iso-prostaglandin F2α in pericardial fluid of patients with heart failure: a potential role for *in vivo* oxidant stress in ventricular dilatation and progression to heart failure. *Circulation* **97,** 1536–1539
25. Landau, B. R., Wahren, J., Chandramouli, V., Schumann, W. C., Ekberg, K., and Kalhan, S. C. (1996) Contributions of gluconeogenesis to glucose production in the fasted state. *J. Clin. Invest.* **98,** 378–385
26. Bock, G., Schumann, W. C., Basu, R., Burgess, S. C., Yan, Z., Chandramouli, V., Rizza, R. A., and Landau, B. R. (2008) Evidence that processes other than gluconeogenesis may influence the ratio of deuterium on the fifth and third carbons of glucose: implications for the use of $^{2}H_2O$ to measure gluconeogenesis in humans. *Diabetes* **57,** 50–55
27. Basu, R., Chandramouli, V., Schumann, W., Basu, A., Landau, B. R., and Rizza, R. A. (2009) Additional evidence that transaldolase exchange, isotope discrimination during the triose-isomerase reaction, or both occur in humans: effects of type 2 diabetes. *Diabetes* **58,** 1539–1543
28. Jones, J. G., Garcia, P., Barosa, C., Delgado, T. C., Caldeira, M. M., and Diogo, L. (2008) Quantification of hepatic transaldolase exchange activity and its effects on tracer measurements of indirect pathway flux in humans. *Magn. Reson. Med.* **59,** 423–429
29. Goodwin, G. W., Cohen, D. M., and Taegtmeyer, H. (2001) [5-^{3}H]Glucose overestimates glycolytic flux in isolated working rat heart: role of the pentose phosphate pathway. *Am. J. Physiol. Endocrinol. Metab.* **280,** E502–508
30. Pfeifer, R., Karl, G., and Scholz, R. (1986) Does the pentose cycle play a major role for NADPH supply in the heart? *Biol. Chem. Hoppe Seyler* **367,** 1061–1068
31. Burns, A. H., and Reddy, W. J. (1977) Hexose monophosphate shunt in isolated cardiac myocytes from normal rats. *Am. J. Physiol.* **232,** E570–573
32. Jin, E. S., Sherry, A. D., and Malloy, C. R. (2009) Evidence for reverse flux through pyruvate kinase in skeletal muscle. *Am. J. Physiol. Endocrinol. Metab.* **296,** E748–757
33. Chandramouli, V., Ekberg, K., Schumann, W. C., Wahren, J., and Landau, B. R. (1999) Origins of the hydrogen bound to carbon 1 of glucose in fasting: significance in gluconeogenesis quantitation. *Am. J. Physiol. Endocrinol. Metab.* **277,** E717–723
34. Malaisse, W. J., Malaisse-Lagae, F., Liemans, V., Ottinger, R., and Willem, R. (1990) Phosphoglucoisomerase-catalyzed interconversion of hexose phosphates: isotopic discrimination between hydrogen and deuterium. *Mol. Cell. Biochem.* **93,** 153–165
35. Taegtmeyer, H. (1984) Six blind men explore an elephant: aspects of fuel metabolism and the control of tricarboxylic acid cycle activity in heart muscle. *Basic Res. Cardiol.* **79,** 322–336
36. Drake, A. J., Haines, J. R., and Noble, M. I. (1980) Preferential uptake of lactate by the normal myocardium in dogs. *Cardiovasc. Res.* **14,** 65–72